Diffusion in concentrated lattice gases. V. Particles with repulsive nearest-neighbor interaction on the face-centered-cubic lattice

R. Kutner,* K. Binder, and K. W. Kehr
Institut für Festkörperforschung der Kernforschungsanlage Jülich, D-5170 Jülich, Postfach 1913, Federal Republic of Germany
(Received 9 February 1983)

The diffusion of particles in concentrated lattice gases is studied by Monte Carlo methods, assuming a fcc lattice with repulsive nearest-neighbor interaction. Particular attention is paid to the influence of ordering on the diffusion properties, since the model has ordered superstructures at low temperatures T near the stoichiometric concentrations $c=\frac{1}{4}$, $\frac{1}{2}$, and $\frac{3}{4}$. Both the self-diffusion of tagged particles and the collective diffusion by which concentration fluctuations decay are obtained. In the ordered regions both diffusivities are rather small due to a strong decrease of the effective jump rate of the particles. The correlation factor $f(T,c)$ for self-diffusion has a pronounced nonmonotonic concentration dependence for low temperatures. This is interpreted by reducing the problem near $T=0$ and the limits $c\to\frac{1}{4}-,\frac{1}{2}-$ to an effective single-vacancy problem, and $c\to\frac{1}{4}+,\frac{1}{2}+$ to an effective single-particle problem. Other lattices are briefly discussed.

I. INTRODUCTION

In the first paper of this series[1] (hereafter referred to as I) we have investigated self-diffusion in a noninteracting fcc lattice gas at arbitrary concentration c of particles. In the second paper[2] (hereafter referred to as II) we then considered the effect of an attractive nearest-neighbor interaction. This model has a critical point at $c=c_{\rm crit}$, $T=T_c$, and separates below the critical temperature into two phases of low and high concentration, respectively. While these static properties are dramatically reflected in the collective diffusion constant, which is strongly decreased in a broad regime of concentrations near the critical point where it ultimately vanishes, they have relatively little effect on the self-diffusion coefficient. The main effect of temperature on self-diffusion is a small reduction of the vacancy availability factor V compared to the noninteracting case, and a slight reduction of the effective jump rate W with which a particle hops to an available empty neighboring site. The correlation factor f which measures the backward correlations inherent in self-diffusion was even found temperature independent within our numerical accuracy.

In the present paper we proceed to the very interesting case of a repulsive interaction between nearest neighbors, which leads to ordering tendency rather than clustering. In fact, this model has been rather popular in modeling ordering phenomena in binary metallic alloys such as the Cu-Au system,[3-19] and has also been considered[20] in the context of models for superionic conductors.[21] Of course, it is clear that for a faithful description of ordering phenomena in all these systems, more complicated interactions than just nearest-neighbor repulsion will be required, e.g., superionic conductors may be modeled instead by lattice gases with Coulomb interactions.[22] Before one can proceed to such more complicated problems, one should first analyze the present system as a useful starting point. In addition, relatively simple models of this type seem to be applicable to metal-hydrogen systems[23] such as Pd-D.[24] Two-dimensional models of this type may be applicable to study order-disorder phenomena in chemisorbed monolayers at surfaces[25] and in intercalation compounds.[26]

The effect of repulsive interactions on diffusion in lattice gases has been considered in previous work by Murch and Thorn.[27-31] Most of their work, however, refers to other lattices (particularly two-dimensional ones[27,29]; the fcc system considered in Ref. 30 is restricted to concentrations $c\leq 0.08$ and a single temperature, in view of a possible application to carbon diffusion in austenite.[32] In addition, as noted by the authors themselves,[27] their Monte Carlo procedures were of rather uncertain validity when the lattice gas is in its ordered regions, and thus they have not attempted to estimate the precise phase diagram of these models. In the present paper we are particularly interested in elucidating the effects of (long-range) order on the diffusion properties of the model system. Making use of the extensive studies by which the static phase diagram has been calculated,[16,17] we carefully prepare equilibrium configurations for the conditions chosen, as described in Sec. II, as initial states for our study of diffusion coefficients. In each region of the phase diagram where the system is ordered, we hence ensure that we work with the system being a monodomain of the phase with the appropriate equilibrium value of the order parameter. Thus we measure even at very low temperatures the bulk diffusivities only, and avoid getting artificial enhancement of diffusivities due to antiphase boundaries or other defects in the structure of the system.

In Sec. III we shall present our numerical results for the effective jump rate W, the tracer-diffusion coefficient D_t, and its correlation factor f as a function of temperature and concentration in detail. Some data for the collective diffusion at low temperatures will also be presented. Section IV then contains a discussion of the limiting behavior of this system as $T\to 0$. It will be shown that near the stoichiometric compositions $\frac{1}{4}$ and $\frac{1}{2}$ (but not $\frac{3}{4}$) the problem can be effectively reduced to the diffusion of a single extra particle (vacancy) on the otherwise perfect lattice of empty (full) sites in the respective structure. Thus the correlation factor at these stoichiometric compositions,

as well as W and D_t themselves, are thereby obtained analytically in the limit of very small T. Section V contains our conclusions, as well as an outlook to other models. A brief comparison to a recent study of surface diffusion in ordered chemisorbed monolayers performed along similar lines[33] will also be made.

II. STATIC PROPERTIES OF THE FCC LATTICE GAS MODEL WITH NEAREST-NEIGHBOR REPULSION AND THE APPROPRIATE PREPARATION OF INITIAL STATES

As usual (see II or Ref. 25, for instance), we use the transcription of the lattice gas to the equivalent problem of a system of Ising spins $\mu_i = \pm 1$ [the plus sign corresponds to either an empty site (lattice gas) or an A atom (binary-alloy terminology) while the minus sign corresponds to either a full site (lattice gas) or a B atom], whenever this is convenient. The problem then corresponds to an antiferromagnet (nearest-neighbor exchange constant J_{NN} negative) on the fcc lattice in a magnetic field H. The phase diagram[16,17] as shown in Fig. 1 involves at

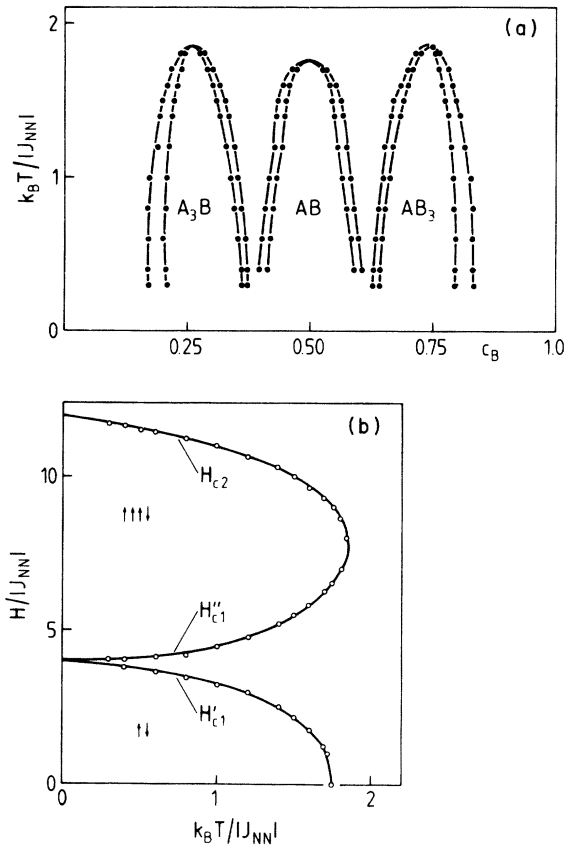

FIG. 1. Phase diagram of the nearest-neighbor face-centered-cubic lattice in the temperature-concentration plane (a) and in the temperature-magnetic field plane (b). Ordered structures are indicated. All transitions are found to be of first order; therefore, in the T-c plane the transition lines are split into two-phase coexistence regions: utmost to the left the disordered phase and A_3B coexist, etc. Solid and open circles are Monte Carlo results obtained as described in Ref. 17, while the curves are only guides to the eye. Varying the field at fixed (low) temperature one crosses phase boundaries at the three critical fields H'_{c1}, H''_{c1}, and H_{c2}.

nonzero temperature then the three ordered structures shown in Fig. 2.[34]

As in I and II, we always start the calculation with a simulation in the (T,H) ensemble (or grand-canonical ensemble of the lattice gas), because its equilibration is quicker than in the (T,c) ensemble (canonical ensemble of the lattice gas) where the convergence is slowed down due to the conservation law.[35] At high temperatures above all transitions (e.g., Fig. 3) it does not matter whether we start this simulation with a state of all spins up (for $H>0$) or all spins down (for $H<0$), or whether we use one of the perfectly ordered spin arrangments or a randomly chosen spin configuration: After a short time both magnetization m, internal energy U, etc., obtain their equilibrium values. By comparing our data to previous work on the same model[16,17] we check the program. Within the statistical scatter the results for m,U, etc., do not depend on the lattice size N (as usual we use periodic boundary conditions throughout). A further check is provided by the symmetry properties $m(-H)=-m(H)$, $U(-H)=U(H)$, which are fulfilled within the statistical error [Figs. 3(a) and 3(b)]. As noted in II the vacancy availability factor V [Fig. 3(c)] is simply related to the nearest-neighbor Cowley short-range order parameter α_1 (Ref. 36) via

$$V=(1-c)(1-\alpha_1) \ . \tag{1}$$

In our model α_1 is symmetric around $c=\frac{1}{2}$, and related to

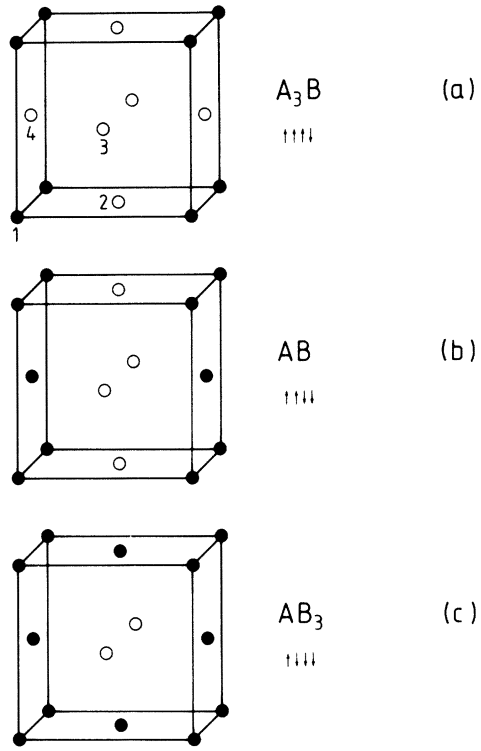

FIG. 2. Unit cells of the ordered structures occurring in the nearest-neighbor face-centered-cubic lattice gas. The lattice is divided into four simple-cubic sublattices 1,2,3,4 in (a). In the structure at $c=\frac{1}{4}$ one sublattice is full, the others are empty (a), at $c=\frac{1}{2}$ two sublattices are full (b) and at $c=\frac{3}{4}$ three sublattices are full (c). The structure notation used in Fig. 1 is also indicated.

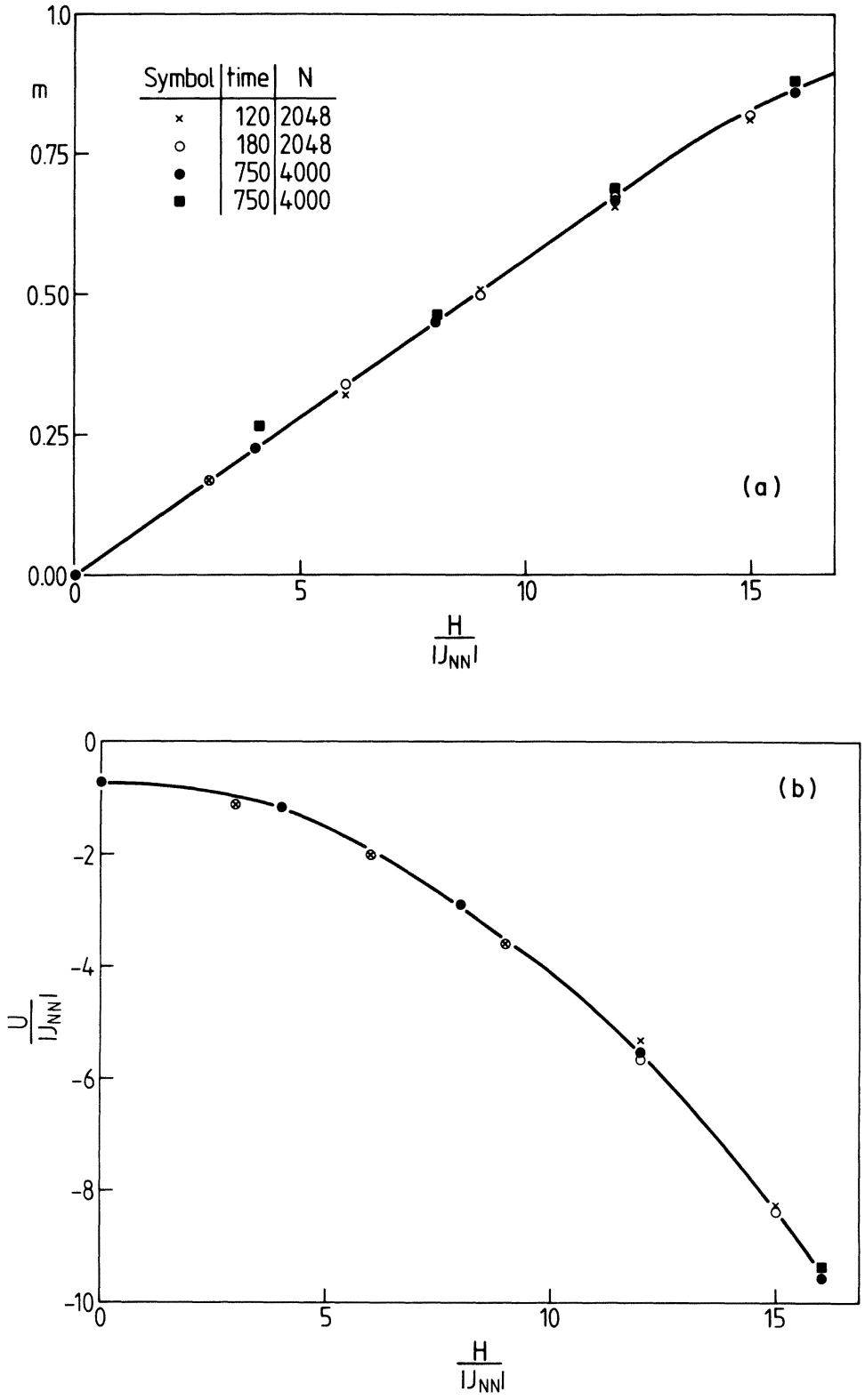

FIG. 3. (a) Magnetization plotted vs field at $k_BT/|J_{NN}|=4$. Time is given in units of Monte Carlo steps (MCS) per site. Solid symbols denote present data, other symbols denote previous work (Refs. 16 and 17). The solid squares actually represent the result for $-m$, obtained for negative fields which must coincide with the result for m at the respective positive fields. Note that in addition to the runs in the grand-canonical ensemble the present data were also averaged over 4000 additional MCS per particle in the canonic ensemble. (b) Internal energy U plotted vs field at $k_BT/|J_{NN}|=4$. Solid squares representing U taken at negative fields are only shown where they not exactly coincided with the data for positive H. (c) Vacancy availability factor plotted vs concentration. The straight line is the result for the noninteracting case, $V=1-c$.

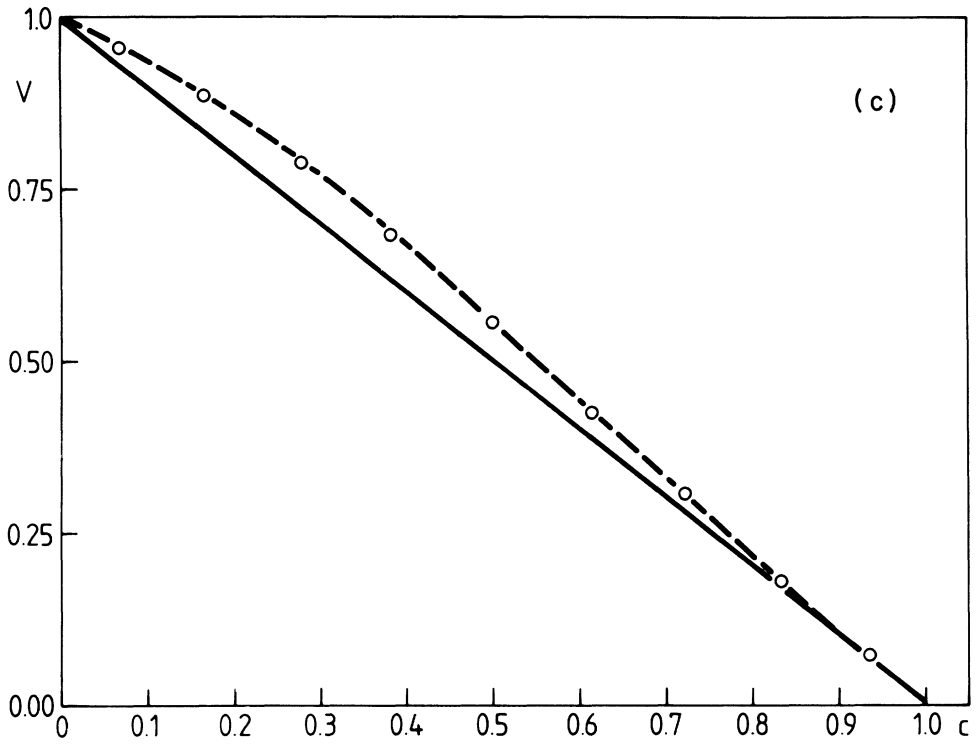

FIG. 3. (*Continued.*)

the internal energy $U(H)$ by[17]

$$24c(1-c)J_{\mathrm{NN}}(1-\alpha_1)=U(H)+mH+6J_{\mathrm{NN}} \ .$$

At high temperatures V is only slightly enhanced over its noninteracting value (α_1 is negative in our model, rather than positive as it was in the attractive case, and hence reflects an ordering rather than clustering tendency).

At low temperatures, however, the behavior is rather different. The magnetization curve $m(H)$ is split into seven distinct branches, which do not join up smoothly but are separated from each other by jump discontinuities occurring at the critical fields $\pm H_{c2}, \pm H'_{c1}, \pm H''_{c1}$ [Fig. 4(a)]. These jump discontinuities correspond to the two-phase regions of Fig. 1. In this case it is absolutely essential to start the system with the appropriate initial condition: either random spin configurations or all spins up for $H > H_{c2}$; A_3B structure for fields in the range $H''_{c1} < H < H_{c2}$; either random spin configurations or all spins up for $H'_{c1} < H < H''_{c1}$; AB structure for fields $-H'_{c1} < H < H'_{c1}$, etc. In this case the system very quickly relaxes to its appropriate thermal equilibrium, and observation times of a few hundred Monte Carlo steps (MCS) per site are sufficient. If one starts with a "wrong" initial condition, one sometimes also manages to relax the system to the same equilibrium state (but one needs "aging times" of several thousand MCS per site), while in other cases the system gets "frozen in" (within the accessible observation times) in metastable states. Inspection of their spin configurations shows that the system then has not reached a uniformly ordered state, but rather several ordered regions separated by domain walls (which sometimes run from one boundary of the system to the opposite one, thus utilizing the periodic boundary conditions). Size and number of domains greatly varies from one run to the next, and hence with such "wrong" initial conditions one gets rather erratic and ill-defined results. Thus such inhomogeneous states are not suitable as initial states for the subsequent diffusion runs, as typically the mobility in the domain walls is largely enhanced, and one hence does not measure bulk behavior even if there are only a few walls in the system. Without characterizing the precise domain arrangement such results would be meaningless.

Of course, the precise values of the critical fields are not known beforehand and must themselves be estimated from the Monte Carlo calculation. This is not straightforward at low temperatures where pronounced hysteresis occurs.[16,17] A reliable method to estimate the critical fields involves estimating the free energies which belong to the various branches in Figs. 4(a) and 4(b), see Ref. 16. The critical fields are then found from the intersection points of the various branches. We think that the uncertainty involved in all these procedures should not exceed the size of the dots shown in Fig. 1.

In the short-range order parameter α_1 the ordered structures show up as rather pronounced peaks [Fig. 5(a)]. As expected, the vacancy availability factor [Fig. 5(b)] is reminiscent of this peak structure. As expected from Fig. 2(a), V stays close to unity for $c \lesssim \frac{1}{4}$ and falls off; it always exceeds the result for the noninteracting case ($V=1-c$) due to the ordering tendency of the particles. Similar data, as shown in Figs. 3, 4, 5(a), and 5(b), have also been obtained at the temperatures $k_BT/|J_{\mathrm{NN}}| = 20,6,5$ (disordered phase) and 1.8, 1.6, 0.8 (displaying ordering behavior). One more example is given in Fig. 5(c).

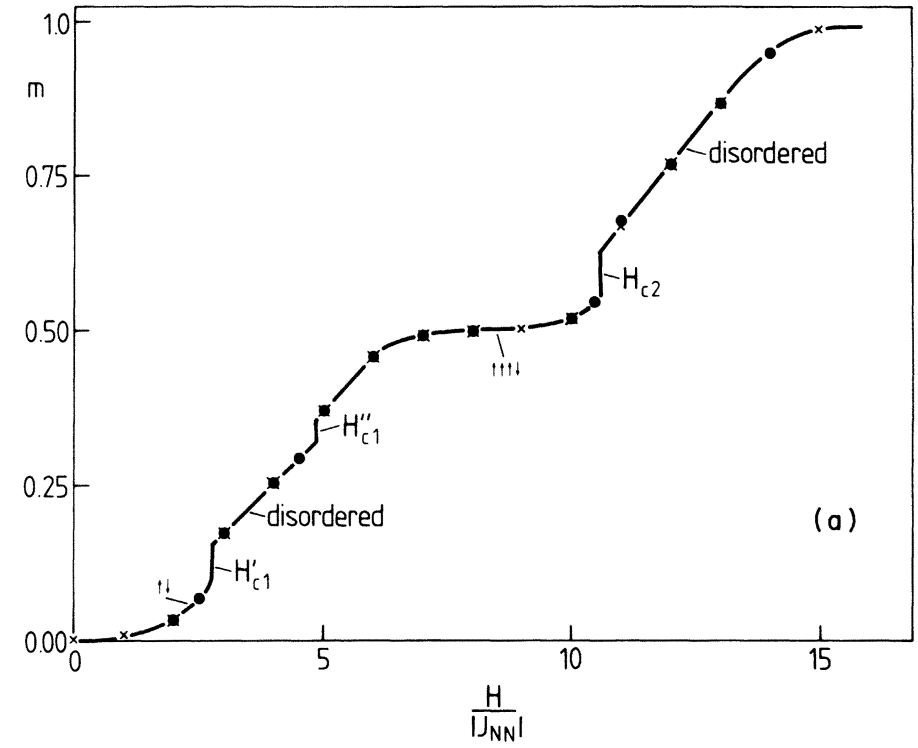

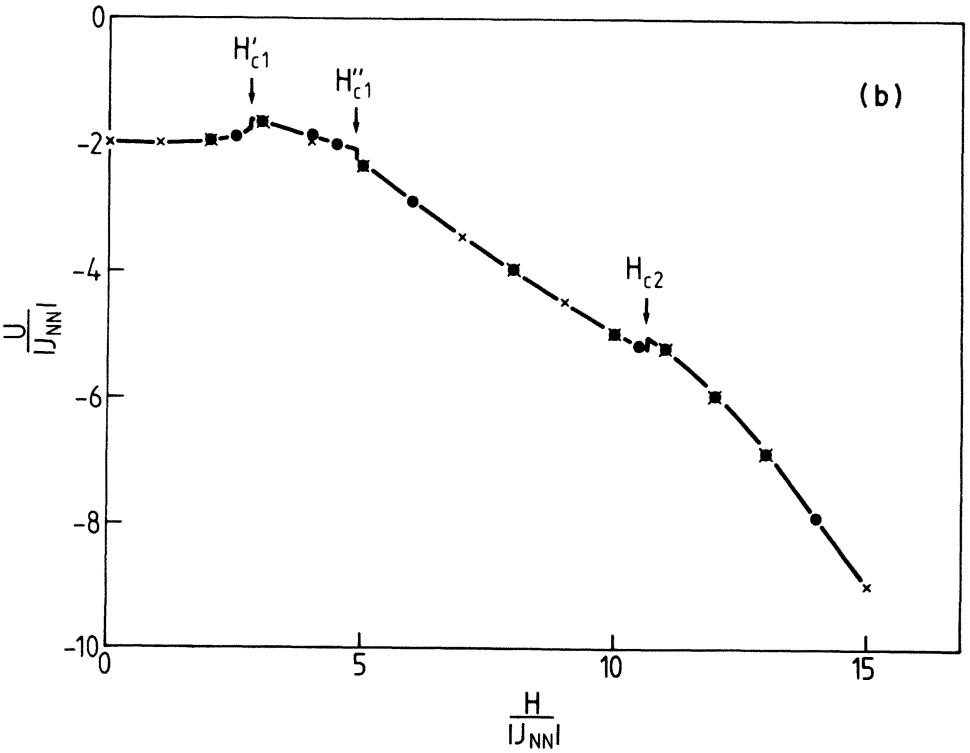

FIG. 4. (a) Magnetization plotted vs field at $k_BT/|J_{NN}|=1.2$, for lattices of size $N=16384$. Crosses are taken from Ref. 16, solid circles are present data. (b) Internal energy U plotted vs field at $k_BT/|J_{NN}|=1.2$. Data for U at negative fields coincide exactly with those for positive ones and hence are not shown. Note that in addition to the runs in the grand-canonical ensemble the present data were also averaged over 1600 MCS per particle in the canonic ensemble.

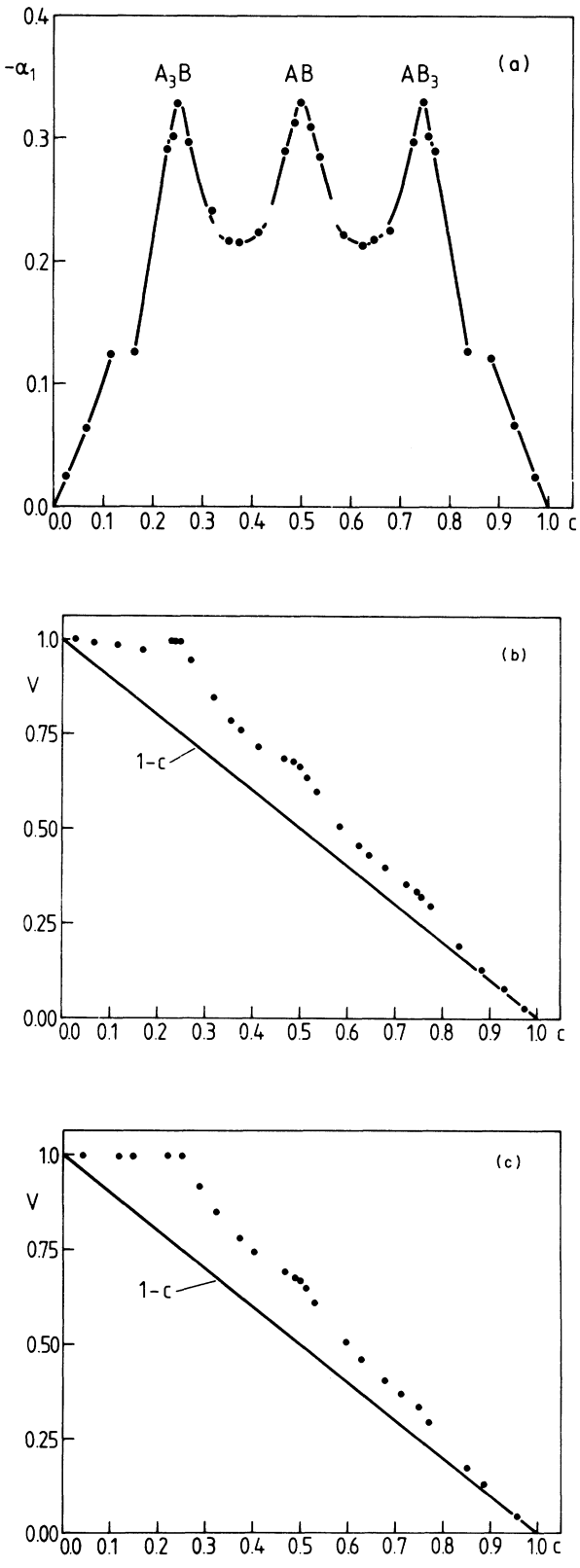

FIG. 5. (a) Short-range order parameter α_1 plotted vs concentration at $k_BT/|J_{NN}|=1.2$. (b) Vacancy availability factor V plotted vs concentration at $k_BT/|J_{NN}|=1.2$. (c) Vacancy availability factor V plotted vs concentration at $k_BT/|J_{NN}|=0.8$.

III. MONTE CARLO SIMULATION OF JUMP RATES, TRACER, AND COLLECTIVE DIFFUSION CONSTANTS

A. General remarks

As in II, we then store some typical equilibrium configurations of the system thus obtained as initial states for a simulation of diffusion. In this second part of the simulation, a particle at site i is chosen at random and then a jump to a randomly selected neighboring site (l_i) is attempted. The attempted jump is actually performed only if a random number ζ, with $0<\zeta<1$, is less than the transition probability $W(\mu_i\to\mu_{l_i})$,

$$W(\mu_i\to\mu_{l_i})=\tfrac{1}{2}[1-\tanh(\delta\mathscr{H}/2k_BT)]\times\delta(\mu_i+1)\delta(\mu_{l_i}-1)\ . \tag{2}$$

Only occupied lattice sites ($\mu_i=-1$) are considered for a jump, and a jump is possible only to a neighboring empty site ($\mu_{l_i}=+1$); these restrictions are taken into account by the two δ functions in (2). The factor in square brackets depends on the energy change $\delta\mathscr{H}$ involved by this jump and ensures the detailed balance condition. For more details about the master equation describing the hopping process see II; here we only recall that the choice for W given in (2) is not at all unique, and differs, in fact, from choices made in related work.[27–31] We have used here the same choice as in our other studies,[2,33] which is convenient as the effective rate W at which possible jumps on the average are performed,

$$W\equiv\tau_s^{-1}\langle W(\mu_i\to\mu_{l_i})\rangle/V \tag{3}$$

becomes symmetric around $c=\frac{1}{2}$, and moreover $\tau_s W\to\frac{1}{2}$ for both $c\to0$, $c\to1$, independent of temperature. Hence in the dilute case (or the case of dilute vacancies) the mobility is never very small, in contrast to other possible choices instead of Eq. (2).

The inverse time-scale factor τ_s^{-1} has been introduced in Eq. (3) to convert probabilities into rates. Of course, as is well known for all Monte Carlo simulations of dynamic processes,[35] there is no intrinsic time scale defined by the Monte Carlo process itself; hence we take as a time unit one MCS per particle. During one MCS per particle each particle attempts once, on the average, to perform a hop. Since there are $z=12$ nearest-neighbor sites on the fcc lattice, the rate of attempted jumps between two specific sites is $1/z=\frac{1}{12}$; i.e., $\tau_s=z$ in these units. In the simulations $z\langle W(\mu_i\to\mu_{l_i})\rangle$ is estimated from the quotient of the number of performed jumps to the number of all attempted jumps. Hence $z\langle W\rangle_T$ is estimated from a time average over all successful hopping attempts.

The hopping dynamics described by Eq. (2) obviously conserves the concentration [or magnetization in the magnetic analog, note $c=(1-m)/2$], while other quantities like the internal energy, order parameters, etc., fluctuate. It is one more check on the selection of initial conditions (and the correctness of the program code) that neither of these quantities changes substantially during the simulation of diffusion, and we actually find that within our statistical errors results obtained from runs in the grand-canonical and canonical ensemble are indistinguishable (cf.

Figs. 3–5). This also implies that finite size effects are not important.

B. Results

We start by discussing the case where the system stays disordered at all compositions, cf. Fig. 3 for corresponding static properties. Figure 6 shows that the effective jump rate W decreases considerably, even at temperatures more than twice the maximal ordering temperature. This is an effect of the nearest-neighbor repulsive interaction, which is much more drastic than corresponding properties in the case of attractive forces (Fig. 6 of II). The total jump rate VW is displayed in Fig. 7, as well as the tracer diffusion constant D_t. This quantity is estimated from studying the mean-square displacement of all the (labeled) particles as a function of time, as explained in I in more detail. The resulting correlation factor f, defined via (a is the lattice constant of the fcc lattice)

$$D_t \equiv VWa^2 f \tag{4}$$

is then shown in Fig. 8. One sees that for small concentrations ($c \approx 0.2$) f is slightly smaller and for large concentrations ($c \approx 0.7$) f is slightly larger than its corresponding value in the noninteracting case (see I and Ref. 37). The deviations hardly exceed the inaccuracy of our estimates for f.

The situation changes drastically in the temperature region where the system may order, Figs. 9–13. It is seen that at the ordered structures near the stoichiometric compositions the mobility of the atoms is nearly zero (Fig. 9). This "freezing out" of the motions is also seen in the total jump rate VW and the tracer diffusion constant (Fig. 10).

Particularly interesting is the behavior of the tracer correlation factor f when ordered structures appear (Figs. 11 and 12). At low temperatures the correlation factor exhibits typical minima below and at the stoichiometric compositions $c = \frac{1}{4}$ and $\frac{1}{2}$ of the ordered phases, followed by values near unity slightly above these compositions. In the next section we will discuss the behavior of the correlation factor at low temperatures near the stoichiometric ordered phases $c = \frac{1}{4}$ and $c = \frac{1}{2}$.

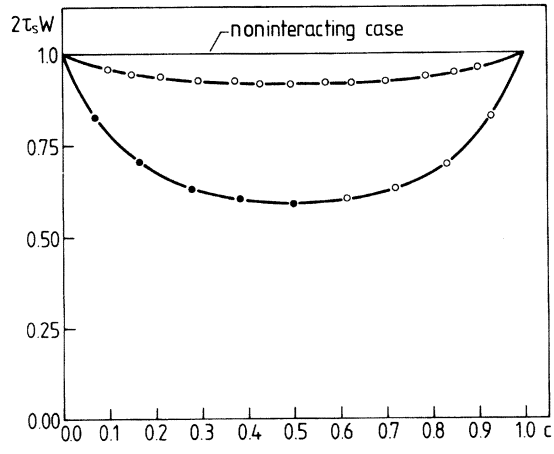

FIG. 6. Effective jump rate W per available empty nearest-neighbor site plotted vs concentration at temperatures $k_BT/|J_{NN}| = 4.0$ (solid circles, data points being based on averages over 4000 MCS per particle in a lattice of 4000 sites) and $k_BT/|J| = 20$ (open circles, based on averages over 1600 MCS per particle in a lattice of 16 384 sites).

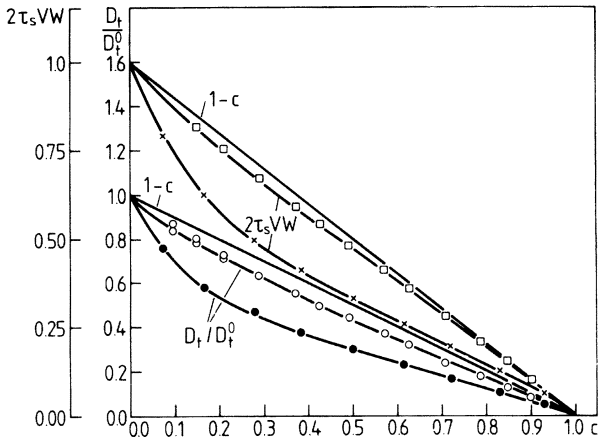

FIG. 7. Total jump rate VW and tracer diffusion coefficient D_t plotted vs concentration at $k_BT/|J_{NN}| = 4$ (solid circles, crosses) and $k_BT/|J_{NN}| = 20$ (open circles, squares), using the data from the same runs on which Figs. 3 and 6 were based. In a few cases two points are shown for the same concentration to indicate the uncertainty resulting from different ways of estimating D_t. D_t is normalized by its value in the noninteracting case as $c \to 0$. Straight lines indicate corresponding "mean-field" prediction $1-c$ in both cases.

Finally we will present some data on the collective diffusion constant at low temperature. While in the disordered region the collective diffusion D is maximal at $c = \frac{1}{2}$, at least in the temperature region far above all transitions, where mean-field approximations are valid as given in II, the small mobility at the stoichiometric concentrations at low temperatures (Fig. 9) also leads to rather small values of D at these concentrations (Fig. 13). In the concentration regions where the system is still disordered, D has pronounced maxima and is larger than its value in the noninteracting case. The results in Fig. 13 are obtained with the "linear-response" technique of II and are somewhat tentative, since better statistics and more concentration values would be required to show the precise behavior near the maxima and minima.

IV. TRACER DIFFUSION NEAR THE STOICHIOMETRIC CONCENTRATIONS $\frac{1}{4}$ AND $\frac{1}{2}$ AT LOW TEMPERATURES

In this section we will relate the observed correlation factor at low temperatures for c slightly less than $\frac{1}{4}$ ($c = \frac{1}{4}-$) or $\frac{1}{2}$ ($c = \frac{1}{2}-$) to a vacancy diffusion process in the ordered structures, and for c slightly larger than $\frac{1}{4}$ ($c = \frac{1}{4}+$) or $\frac{1}{2}$ ($c = \frac{1}{2}+$) to a single-particle diffusion process in the empty positions of the lattice. We begin with $c = \frac{1}{2}$. According to Sec. II and Fig. 1, the ordered structure at $c = \frac{1}{2}$ and very low temperature consists of alternatively filled and empty planes, perpendicular to a [100] direction. The excitation of a particle out of the plane and the concomitant creation of a vacancy requires an extra energy of $3|J|$, the separation of the particle-

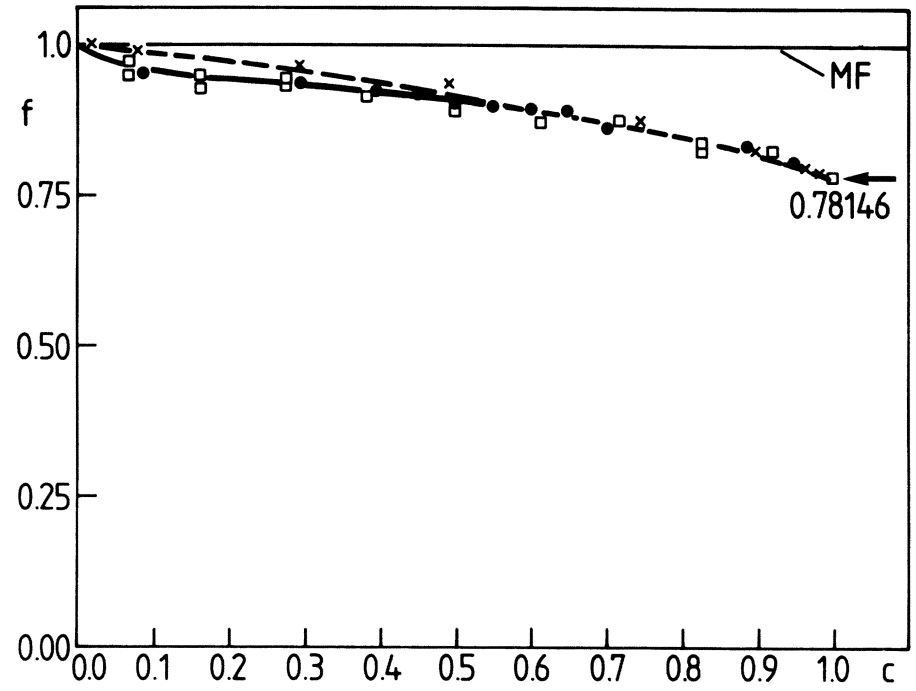

FIG. 8. Tracer correlation factor $f(T,c)$ plotted vs concentration at $k_BT/|J_{NN}|=4$ (squares), 6 (dots), and 20 (crosses). The "mean-field" prediction $f(T,c)=1$ as well as the result of Sankey and Fedders (Ref. 37) (dashed curve), which is an accurate theory for the noninteracting case (see I), are included for comparison. The exactly known limit $f(T,c\rightarrow 1)$ is indicated also. The solid curve is a guide to the eye only.

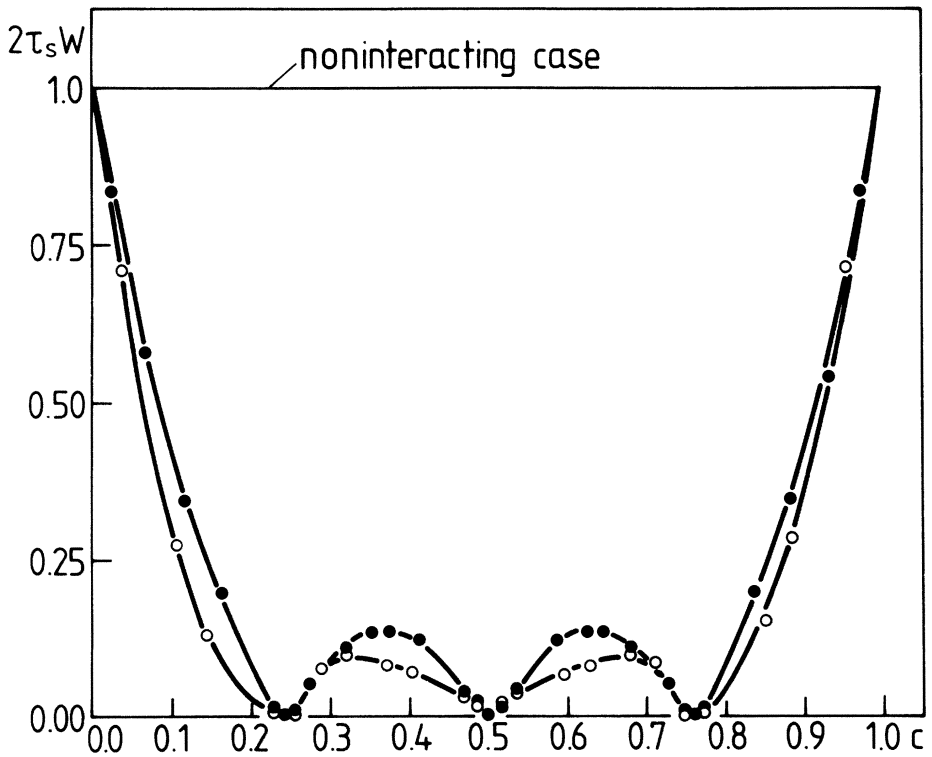

FIG. 9. Effective jump rate W per available empty nearest-neighbor site plotted vs concentration at temperatures $k_BT/|J_{NN}|=1.2$ (solid circles, data being based on averages over at least 1600 MCS per particle in a lattice of 16384 sites) and $k_BT/|J_{NN}|=0.8$ (open circles). For simplicity the small two-phase regions (where jump singularities occur from one phase to the next) are ignored in drawing a unique smooth curve through all points to guide the eye.

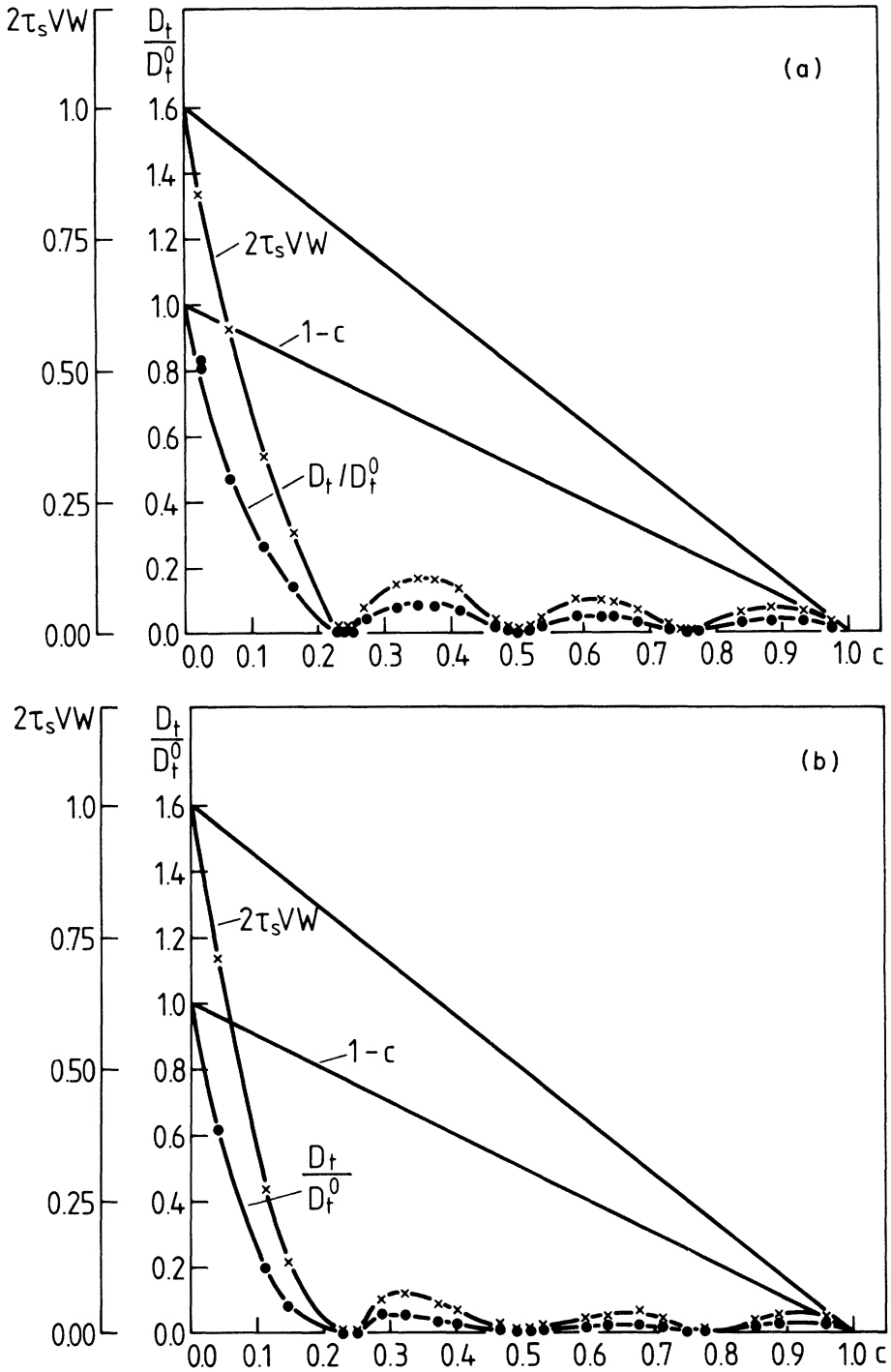

FIG. 10. Total jump rate VW and tracer diffusion coefficient D_t plotted vs concentration at $k_BT/|J_{NN}|=1.2$ (a) and 0.8 (b). D_t is normalized by its value in the noninteracting case as $c\to 0$. Straight lines indicate corresponding mean-field predictions $1-c$ in both cases.

vacancy pair another energy unit $|J|$. Hence this process is unlikely at low temperatures. For concentrations slightly less than $\frac{1}{2}$, we have vacancies in the otherwise filled planes and no extra particles in the empty planes at low T. No energy change is involved in the exchange processes of a vacancy with particles within the planes, at low vacancy concentrations. The diffusion of tagged particles, which are restricted to the planes, is effected by the vacancy process, i.e., the exchange of vacancies with the tagged particles. We have verified in our simulations that at $c=\frac{1}{2}-$ and $k_BT/|J|=0.8$ the diffusion is indeed two dimensional to a very good approximation. The value of the correlation factor for tracer diffusion in a simple-square lattice is exactly known in the limit of vanishing vacancy

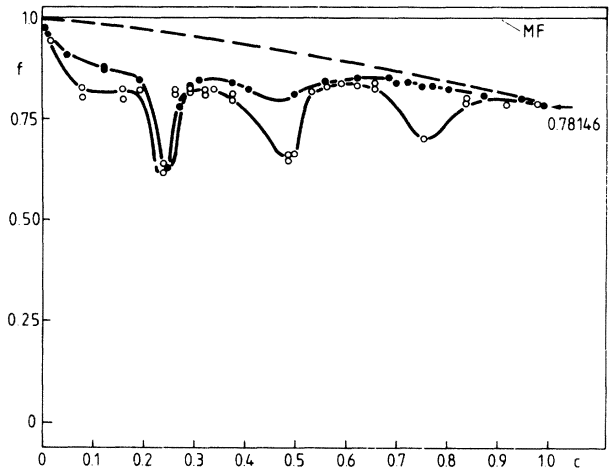

FIG. 11. Tracer correlation factor $f(T,c)$ plotted vs concentration at $k_BT/|J_{NN}|=1.8$ (solid circles) and $k_BT/|J_{NN}|=1.6$ (open circles). For further explanations see Fig. 12.

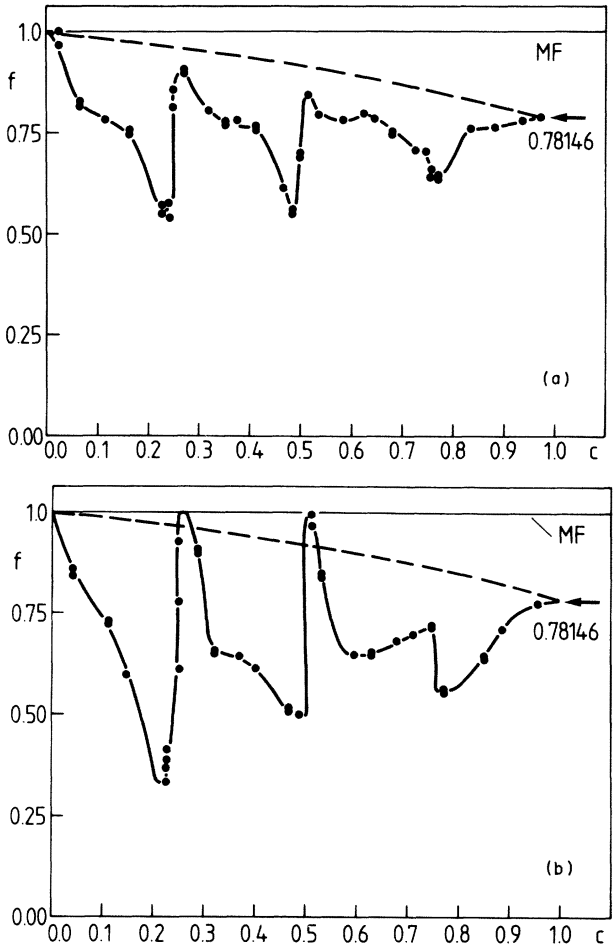

FIG. 12. Tracer correlation factor $f(T,c)$ plotted vs concentration at $k_BT/|J_{NN}|=1.2$ (a) and $k_BT/|J_{NN}|=0.8$ (b). The mean-field prediction $f(T,c)=1$ as well as the result of Sankey and Fedders (Ref. 37) (broken curve) for the noninteracting case are included. The exactly known limit $f(T,c\to 1)$ is indicated also. In a few cases several points are shown for the same concentration to indicate that the data are quite accurate at off-stoichiometric compositions, while the larger scatter at or close to stoichiometry reflects the singular behavior which occurs there for $T\to 0$ (Sec. IV).

concentration,[38] $f=0.466\,942\ldots$. Our simulations show a value of approximately 0.5 at $k_BT/|J|=0.8$ [cf. Fig. 12(b)], in agreement with this consideration. At lower concentrations f increases. In the noninteracting two-dimensional lattice gas $f(c)$ increases approximately linearly with vacancy concentration towards $f=1$ at $c=0$. The measured behavior below $c=\frac{1}{2}$ is consistent with this, although we cannot clearly resolve the precise behavior. Also, near $c=\frac{1}{4}+$ other effects come into play. Slightly above $c=\frac{1}{2}$ we expect the diffusion to be produced by the extra particles which are found between the planes. Again we have checked the two-dimensional nature of diffusion at $c=\frac{1}{2}+$. The correlation factor for self-diffusion of tagged particles at low concentration is unity, in agreement with the findings of the simulation [cf. Fig. 12(b)].

The situation around $c=\frac{1}{4}$ is more difficult to analyze. At $c=\frac{1}{4}$ and very low temperatures we have an ordered structure which forms a simple cubic (sc) lattice with lattice constant a. The creation of a vacancy-particle pair requires $3|J|$, the separation of the extra particle, and the vacancy requires another $|J|$. Hence both processes become extremely improbable at very low temperatures and we can neglect them in the limit $T\to 0$. For c slightly less than $\frac{1}{4}$ ($c=\frac{1}{4}-$) we have permanent vacancies in the sc lattice at $T=0$. In this case, and at very low temperatures, a vacancy-mediated diffusion process will take place in the sc lattice, with apparent nearest-neighbor and second-neighbor transitions of the vacancy of equal rates. As indicated in Fig. 14 a particle which is either a first or second neighbor of the vacancy (counted in the sc lattice) can first jump to an interstitial site of the sc lattice (empty site of the fcc lattice) and then into the vacant site. The first step of this process requires an activation energy of $2|J|$, the second step occurs without activation. Of course, the second step can also lead the particle back to its original site.

We now consider the effective rate $\langle W\rangle_T$ resulting from this two-step process. As mentioned in the preceding section $\tau_s^{-1}\langle W\rangle_T$ is determined from the average of the waiting times between the jumps of the particles. The mean waiting time of a two-step Poisson process with rates Γ_1 and Γ_2 is $\bar{t}=\Gamma_1^{-1}+\Gamma_2^{-1}$. Since the two steps are counted as two events,

$$\tau_s^{-1}\langle W\rangle_T \propto 2(\Gamma_1^{-1}+\Gamma_2^{-1}) \ . \tag{5}$$

In our case $\Gamma_1=\Gamma\exp(-2|J|/k_BT)$ and $\Gamma_2=\Gamma$, hence

$$\tau_s^{-1}\langle W\rangle_T=\frac{2\Gamma}{\exp(2|J|/k_BT)+1}V_{\text{app}} \ . \tag{6}$$

V_{app} is the apparent vacancy availability factor in the sc lattice which determines the probability that a chosen particle can actually perform the two-step process under consideration. In the limit of very low temperatures, $\tau_s^{-1}\langle W\rangle_T\approx 2\Gamma_1 V_{\text{app}}$. The same results can be derived from the ensemble average of the rates by taking the con-

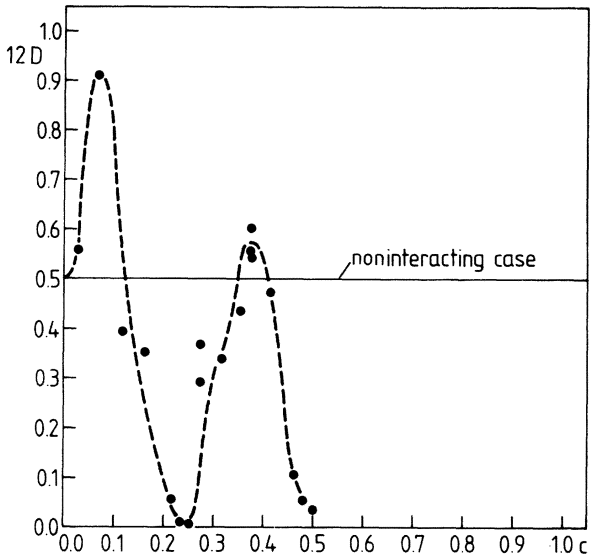

FIG. 13. Collective diffusion constant plotted vs concentration at $k_BT/|J_{NN}|=1.2$. (Since D is symmetric around $c=\frac{1}{2}$ in our case, only data for $c\leq\frac{1}{2}$ were taken.) Each point is an average over four independent runs where the decay of a concentration wave was watched over 80 MCS per particle. At some concentrations several such averages have been taken and are shown separately to give a feeling of the statistical accuracy.

dition of detailed balance into account. The question of whether the process discussed above only contributes to $\tau_s^{-1}\langle W\rangle_T$ or whether other processes are also important, can be examined by comparing the simulations of $\tau_s^{-1}\langle W\rangle_T$ at $c=\frac{1}{4}-$ with Eq. (6).

Since Eqs. (5) and (6) include return processes of the particle to the original site, the apparent transition rate of the vacancy to first and second neighbors in the sc lattice must be considered separately. The particle jumps in two steps either directly to the vacant site, or after the first step it makes one or several returns to the starting site before it performs the final transition. Resummation of the resulting series leads to a distribution of waiting times with mean value $\bar{t}=(\Gamma_1^{-1}+2\Gamma_2^{-1})$. Using the expressions for Γ_1,Γ_2 given above we have the apparent rate

$$\tau_s^{-1}\langle W_{\rm app}\rangle=\frac{\Gamma}{\exp(2|J|/k_BT)+2}V_{\rm app}\ . \tag{7}$$

In the limit of very low temperatures, $\tau_s^{-1}\langle W_{\rm app}\rangle\approx\Gamma_1 V_{\rm app}$. This result is physically plausible, since Γ_1 is the rate-limiting step for the apparent transitions near $T=0$.

The correlation factor for self-diffusion of tagged particles at $c=\frac{1}{4}-$ cannot be taken from the literature, since the vacancy jumps include first- and second-neighbor transitions. It is straightforward to extend existing derivations to this case, and we follow the formulation of Montet.[38] For small apparent vacancy concentration on the sc lattice, f is given by correlations of consecutive jumps only,

$$f=\frac{1+\langle\cos\theta\rangle}{1-\langle\cos\theta\rangle}$$

and

$$\langle\cos\theta\rangle=\lim_{n\to\infty}\frac{\sum_{i=1}^{n}\vec{r}_i\cdot\vec{r}_{i+1}}{\sum_{i=1}^{n}\vec{r}_i^{\,2}}\ , \tag{8}$$

where $\vec{r}_i$ is the jump vector of jump number i of a tagged particle. The denominator of Eq. (8) includes contributions from nearest- and next-nearest-neighbor jumps. In the numerator of Eq. (8) the four contributions from successive first-to-first, second-to-second, first-to-second, and second-to-first neighbor jumps must be considered separately. The average of the cosine is determined by the expectation to find the vacancy at one of the final sites after two successive steps, combined with elementary geometrical considerations. The expectation of finding the vacancy is given by the Green's function $P(i,j,k)$ for diffusion on a sc lattice, cf. Montet[38] for its definition. The final expression is

$$\begin{aligned}\langle\cos\theta\rangle=\tfrac{1}{72}[&P(2,2,0)+2P(2,1,1)+8P(2,1,0)\\&+4P(2,0,0)-2P(1,1,0)-8P(1,0,0)\\&-5P(0,0,0)]\ .\end{aligned} \tag{9}$$

A numerical evaluation of the combination of the Green's functions appearing in Eq. (9) yields

$$\langle\cos\theta\rangle=-0.105\,586\ldots$$

and (10)

$$f=0.808\,996\ldots\ .$$

Finally we compare the results of these derivations with the simulations. Figure 12(b) shows that the correlation factor approaches a value of about 0.4 at the lowest temperature investigated and $c=\frac{1}{4}-$; hereby f has been determined by using the formula Eq. (4) $D_t=\tau_s^{-1}\langle W\rangle_T a^2 f$. For apparent diffusion on the sc lattice,

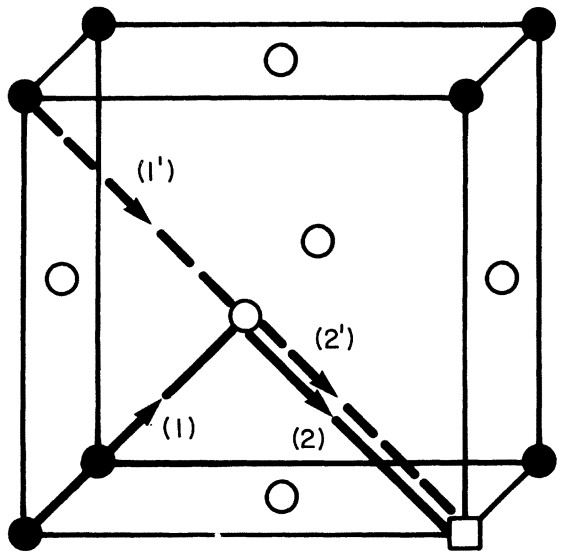

FIG. 14. Two-step processes of particles in the sc lattice at $c=\frac{1}{4}-$ leading to effective nearest- and second-neighbor jumps of a vacancy.

the appropriate expression is

$$D_t = \tau_s^{-1} \langle W_{\text{app}} \rangle a^2 f_{\text{app}} \ .$$

Since at low temperatures $\langle W_{\text{app}} \rangle \approx \frac{1}{2} \langle W \rangle_T$, we have $f_{\text{app}} \approx 2f$, or from the results of the simulations, $f_{\text{app}} \approx 0.8$. There is good agreement with the derivations given above.

At $c = \frac{1}{4} +$ and low temperatures the correlation factor approaches 1, in agreement with a dominant single-particle diffusion process. We have also checked at both $c = \frac{1}{4} -$ and at $c = \frac{1}{4} +$ that the diffusion process was truly three dimensional.

V. CONCLUSIONS

In this paper we have complemented our previous studies of self-diffusion (and collective diffusion) in fcc lattice gases with no interactions (I) or attractive interactions (II) by now also considering repulsive interactions. From these studies the following general conclusions emerge.

(i) At high enough temperatures where the system is distinctly above any phase transitions at all concentrations, the tracer correlation factor f is not very different from the noninteracting case. The effective jump rate W of atoms per available empty nearest-neighbor site decreases both for repulsive and attractive interactions. In our model W is symmetric around $c = \frac{1}{2}$, and hence this decrease is most pronounced for this composition; the decrease is also more drastic for the repulsive interaction case, since there the regime of the disordered phase extends to much lower temperatures (on the scale of the interaction strength $|J|$) than for the case of attractive interactions. In contrast, the vacancy availability factor behaves quite differently in both cases, since $V = (1-c)(1-\alpha_1)$ and already the sign of the short-range order parameter α_1 is different. While V then decreases rather quickly with increasing concentration for attractive interactions where $\alpha_1 > 0$, we find that V is nearly unity up to the concentration where (at low temperatures) the first stoichiometric structure appears in the model with repulsive interactions. The self-diffusion constant ($D_t = VWa^2 f$) then decreases rather rapidly with concentration, both in the repulsive and attractive case, but it stays finite and nonzero even at phase transition points. In contrast, the collective diffusion constant decreases with concentration in the attractive case (and even vanishes at the critical point), while it becomes enhanced over its noninteracting value in the repulsive case.

(ii) At low temperatures, for attractive interactions most concentrations would fall in the "forbidden" region of two-phase coexistence. Outside of the coexistence curve, one is then either in the dilute regime ($c \ll 1$) or in the regime where vacancies are very dilute ($1-c \ll 1$), and then the situation is not so different from the case described above, since $W(c \to 0) \to 1$, $W(c \to 1) \to 1$, $\alpha_1(c \to 0) \to 0$, $\alpha_1(c \to 1) \to 0$, $f(c \to 0) = 1$, $f(c \to 1) = 0.781\,46$, independent of temperature, and hence the effects of the interactions are not very important.

For low temperatures and repulsive nearest-neighbor interactions, the situation is quite different. In the fcc lattice, three ordered structures appear at the stoichiometric concentrations $c = \frac{1}{4}, \frac{1}{2}, \frac{3}{4}$, and there at low temperatures W vanishes exponentially fast, while in the disordered regions around $c \approx \frac{3}{8}$, $\frac{5}{8}$, as well as for $c \lesssim \frac{1}{6}$, $c \gtrsim \frac{5}{6}$, pronounced atomic mobility persists down to very low temperatures. As a consequence, while observing W as function of c at a fixed low temperature, we see that pronounced minima of W occur at the stoichiometric compositions. These minima are also seen in the self-diffusion constant and the collective diffusion constant; while the latter has rather sharp maxima in the disordered regions ($c \lesssim \frac{1}{6}$, $c \approx \frac{3}{8}$, $c \approx \frac{5}{8}$, $c \gtrsim \frac{5}{6}$), the height of these peaks exceeding even the diffusion in the noninteracting case, the self-diffusion constant is also nonmonotomic but stays very small at all compositions exceeding $c \gtrsim \frac{1}{6}$.

(iii) A particular interesting behavior occurs at low temperatures in the ordered structures at slightly off-stoichiometric compositions; e.g., for $c = \frac{1}{2}$ the perfectly ordered crystal is an array where completely filled and completely empty planes (parallel to each other and oriented in a cubic lattice direction) alternate. For $c = \frac{1}{2} +$ the excess concentration is due to a few excess particles in the otherwise empty planes, and hence the correlation factor tends to unity and the self-diffusion is dominated by the free motion of these excess atoms in their planes. As a consequence, the diffusion is very anisotropic; directions parallel and perpendicular to the planes are not equivalent. Such an anisotropy of diffusion due to symmetry-breaking of an ordered structure was also found in studies of models for surface diffusion in ordered monolayers.[33] In the limit of vanishing temperature the space dimensionality in which self-diffusion takes place is reduced by 1. For $c = \frac{1}{4} +$, on the other hand, although the mobility is again due to the excess atoms, and $f \to 1$, the different character of the ordered structure still allows a truly three-dimensional diffusion, there is neither anisotropy nor dimensionality reduction. At $c = \frac{3}{4} +$, finally, the mobility of excess particles is not better than the mobility of the atoms in the stoichiometric structure, and indeed there is no numerical evidence that $f \to 1$ there. These comments already indicate that there is no completely general rule for what happens near stoichiometric structures; rather each structure has to be considered separately. But note that we do expect similar anisotropy of diffusion and effective lowering of dimensionality for all layered structures where n full and m empty planes alternate with n,m integers ≥ 1, i.e., also for other lattices (simple cubic, body-centered-cubic, etc.), and we expect this to occur for much wider classes of interactions than the present nearest-neighbor repulsion (the only restriction is that the interactions must have a layered structure in the ground state; on the square lattice, for instance, this requires nearest- and next-nearest-neighbor interaction to be sufficiently repulsive,[33] a nearest-neighbor repulsive interaction alone would not do).

Similar to this reduction to an effective one-particle problem, the cases $c = \frac{1}{2} -$ and $c = \frac{1}{4} -$ could be reduced to a one-vacancy problem, for which the correlation factor then has also been obtained exactly in terms of lattice Green's functions. Again we expect that reasoning along similar lines as presented in our case will be possible for other ordered structures as well.

*Present and permanent address: Institute of Experimental Physics, Warsaw University, Hoza 69, PL-00-681 Warsaw, Poland.

[1]K. W. Kehr, R. Kutner, and K. Binder, Phys. Rev. B 23, 4931 (1981).

[2]R. Kutner, K. Binder, and K. W. Kehr, Phys. Rev. B 26, 2967 (1982).

[3]W. Shockley, J. Chem. Phys. 6, 130 (1938).

[4]Y. Y. Li, J. Chem. Phys. 17, 449 (1949).

[5]P. W. Anderson, Phys. Rev. 79, 705 (1950).

[6]J. M. Luttinger, Phys. Rev. 81, 1015 (1951).

[7]A. Danielian, Phys. Rev. Lett. 6, 670 (1961); Phys. Rev. A 133, 1344 (1964).

[8]P. C. Clapp and S. C. Moss, Phys. Rev. 171, 754 (1968); 171, 764 (1968); 172, 418 (1968).

[9]M. J. Richards and J. W. Cahn, Acta Metall. 19, 1263 (1971).

[10]S. M. Allen and J. W. Cahn, Acta Metall. 20, 423 (1972); Scr. Metall. 7, 1261 (1973).

[11]N. S. Golosov, L. E. Popov, and L. Y. Pudan, J. Phys. Chem. Solids 34, 1149 (1973); 34, 1159 (1973).

[12]R. Kikuchi and H. Sato, Acta Metall. 22, 1099 (1974).

[13]R. Kikuchi, J. Chem. Phys. 60, 1071 (1974).

[14]M. K. Phani, J. L. Lebowitz, M. H. Kalos, and C. C. Tsai, Phys. Rev. Lett. 42, 577 (1979); M. K. Phani, J. L. Lebowitz, and M. H. Kalos, Phys. Rev. B 21, 4027 (1980).

[15]O. J. Heilmann, J. Phys. A 13, 1803 (1980); S. Alexander and P. Pincus, J. Phys. A 13, 263 (1980).

[16]K. Binder, Phys. Rev. Lett. 45, 811 (1980); Z. Phys. B 45, 61 (1981).

[17]K. Binder, J. L. Lebowitz, M. K. Phani, M. H. Kalos, Acta Metall. 29, 1655 (1981).

[18]U. Gahn, J. Phys. Chem. Solids 43, 977 (1982).

[19]For a general review of the use of lattice-gas models in relation to alloys, see D. de Fontaine, in *Solid State Physics,* edited by H. Ehrenreich, F. Seitz, and D. Turnbull (Academic, New York, 1979), Vol. 34, p. 73.

[20]G. D. Mahan and F. H. Claro, Phys. Rev. B 16, 1168 (1977).

[21]A. Bunde, D. K. Chaturvedi, W. Dieterich, Z. Phys. B 47, 209 (1982); D. K. Chaturvedi and W. Dieterich, Z. Phys. B 49, 17 (1982).

[22]For general reviews on superionic conductors, see *Physics of Superionic Conductors,* edited by M. B. Salamon (Springer, Berlin, 1979); W. Dieterich, P. Fulde, and I. Peschel, Adv. Phys. 29, 527 (1980).

[23]For a general review, see *Hydrogen in Metals I,* edited by G. Alefeld and J. Völkl (Springer, Berlin, 1978).

[24]R. A. Bond and D. K. Ross, J. Phys. F 12, 597 (1982), and unpublished.

[25]For reviews, see M. Schick, Prog. Surf. Sci. 11, 245 (1981); K. Binder, W. Kinzel, and D. P. Landau, Surf. Sci. 117, 232 (1982).

[26]For a review, see *Physics of Intercalation Compounds,* edited by L. Pietronero and E. Tosatti (Springer, Berlin, 1981).

[27]G. E. Murch and R. J. Thorn, Philos. Mag. 35, 493 (1977).

[28]G. E. Murch and R. J. Thorn, J. Phys. Chem. Solids 38, 789 (1977).

[29]G. E. Murch, Philos. Mag. 43, 871 (1981); Solid State Ionics 5, 117 (1981).

[30]G. E. Murch and R. J. Thorn, J. Phys. Chem. Solids 40, 389 (1979).

[31]G. E. Murch, Philos. Mag. 41, 157 (1980).

[32]D. C. Parris and R. B. McLellan, Acta Metall. 24, 523 (1976).

[33]A. Sadiq and K. Binder, Surf. Sci. (in press).

[34]At zero temperature there exists a degeneracy with some other types of structures (Refs. 9 and 10), some of which would be stabilized at nonzero temperature as well by a next-nearest-neighbor repulsion. The present structures are the only ones possible when the next-nearest-neighbor interaction is attractive; however, see Ref. 16. Gahn (Ref. 18 and private communication) claims that there occur order-disorder transitions also near $c \approx \frac{3}{8}$ and $c \approx \frac{5}{8}$, which—if they occur—most probably are some sort of long period superstructures. The phase diagram shown here implies that at (or near) these concentrations the disordered phase reaches down to the ground state, and hence there should be only short-range order.

[35]K. Binder, in *Monte Carlo Methods in Statistical Physics,* edited by K. Binder (Springer, Berlin, 1979), p. 1.

[36]J. M. Cowley, Phys. Rev. 77, 669 (1950); D. T. Keating and B. E. Warren, J. Appl. Phys. 22, 286 (1951).

[37]O. F. Sankey and P. A. Fedders, Phys. Rev. B 18, 5938 (1978).

[38]G. L. Montet, Phys. Rev. B 7, 650 (1973).